

**EFFECT OF FOUNDATION GEOMETRY ON  
SHORT ABUTMENT SCOUR**

by

**REZA MOHAMMADPOUR GHALATI**

**Thesis submitted in fulfilment of the requirements  
for the degree of Doctor of Philosophy**

**November 2012**

## ACKNOWLEDGMENTS

First and foremost, all praise to the Great GOD for His blessings and merciful that enabled me to learn.

I would like to express my deepest appreciation to my supervisor, Professor Dr. Aminuddin Ab. Ghani for his constructive inspiration and invaluable guidance. I really was honoured to have the opportunity to work under his supervision.

I would like to extend my sincere gratitude to Associate Professor Dr. H. Md. Azamathulla for his advice and concern through my study.

Special thanks go to Malaysia country and Director of River Engineering and Urban Drainage Research Centre (REDAC), Professor Nor Azazi Zakaria, for giving me the opportunity to continue my study in Universiti Sains Malaysia. I also would like to acknowledge all the technical staffs in REDAC in assisting me in laboratory and field work.

Last but not least, I am grateful to my dear family specially my parents, Mr. Farhad Mohammadpour and Mrs. Zahra Zaree, who are always my source of inspiration and encouraged me to learn and supported me throughout my life. My deep and most heart-felt gratitude to my brother, sisters for their endless love and support, I would like to dedicate this thesis to my family.

## TABLE OF CONTENTS

Acknowledgments .....	ii
Table of contents .....	iii
List of tables .....	viii
List of figures .....	xiv
List of symbols .....	xxiv
List of abbreviation .....	xxix
Abstrak .....	xxxii
Abstract .....	xxxiii
CHAPTER 1 INTRODUCTION	
1.1 Background.....	1
1.2 Problem Statement.....	5
1.3 Objectives of the Investigation.....	8
1.4 Scope of Present Study .....	9
1.5 Thesis outline.....	9
CHAPTER 2 LITERATURE REVIEW	
2.1 Introduction .....	11
2.2 Sediment Transport in Rivers.....	12
2.2.1 Uniform Non-cohesive Sediments.....	12
2.2.2 Non-uniform and Non-cohesive Sediments.....	15
2.2.3 Cohesive Sediments.....	16
2.3 Type of Bridge Scour .....	17
2.4 Classification of Local Scour around Abutments.....	19
2.5 Short Abutment and Long Abutment .....	22
2.6 Mechanisms of Scour around Abutments.....	23

2.7	Effect of Parameters on Abutment Scour .....	27
2.7.1	Approach Flow Velocity ( $U/U_c$ ) .....	29
2.7.2	Flow shallowness ( $y/L$ ).....	31
2.7.3	Contraction Ratio and Abutment Length.....	33
2.7.4	Sediment Characteristics .....	34
2.7.5	Abutment Shape.....	37
2.7.6	Abutment Alignment .....	38
2.7.7	Channel Geometry .....	39
2.7.8	Time Variation of Scour .....	43
2.8	Equilibrium Time Scour at Abutments.....	48
2.9	Prediction of Maximum Scour Depth at Abutments .....	49
2.9.1	Laursen's Equation .....	50
2.9.2	Liu's Equation .....	50
2.9.3	Gill's Equation.....	51
2.9.4	Sturm and Janjua's Equation .....	52
2.9.5	Froehlich's Equation.....	54
2.9.6	Melville's Equation .....	54
2.9.7	Lim's Equation .....	55
2.9.8	Kandasamy and Melville's Equation.....	58
2.9.9	Chang and Davis's Equation .....	58
2.9.10	Cardoso and Bettess's Equation .....	59
2.9.11	Richardson and Davis's Equation (HIRE Equation) .....	59
2.9.12	Kothyari and Raju's Equation .....	60
2.9.13	Dey and Barbhuiya's Equation.....	62
2.9.14	Fael et al.'s Equation .....	63
2.9.15	Briaud et al.'s Equation .....	64
2.9.16	Ettema et al.'s Equation.....	66
2.9.17	Classification and limitation of Scour Depth Equations.....	69
2.10	Complex Piers Scour .....	71
2.10.1	Jones et al.'s Approach.....	72
2.10.2	Parola et al.'s Approach.....	75
2.10.3	Melville and Raukivi's Approach.....	78
2.10.4	Coleman's Approach .....	80

2.10.5	Sheppard's Approach.....	84
2.10.6	Ashtiani's Approach.....	89
2.10.7	Complex Pier Summary.....	93
2.11	Application of Soft Computing Technique to Predict Local Scour	
	Depth.....	95
2.11.1	Artificial Neural Networks approach.....	95
2.11.2	Genetic programming approach.....	107
2.12	Physical Model.....	113
2.13	Summary.....	115

### CHAPTER 3 MATERIALS AND METHODS

3.1	Introduction.....	116
3.2	Simple Rectangular Channel.....	116
3.2.1	Sand Recess and Bed Materials.....	120
3.2.2	Physical Simulation and Abutment Shapes.....	124
3.2.3	Uniform Flow Conditions.....	129
3.2.4	Threshold Shear Stress and Velocity of the Bed Material.....	134
3.2.5	Data Collection.....	135
3.2.6	Test Duration.....	139
3.2.7	Experiment Procedure.....	139
3.3	Equation Development Techniques.....	142
3.3.1	Regression Analysis.....	142
3.3.2	Artificial Neural Networks (ANNs).....	146
3.3.3	Evolutionary Algorithms.....	150
3.3.4	Genetic Programming (GP).....	151
3.3.5	Performance Measures.....	158

### CHAPTER 4 LOCAL SCOUR AROUND UNIFORM ABUTMENT

4.1	Introduction.....	160
4.2	Dimensional Analysis.....	160
4.3	Equilibrium Scour Depth and Experimental Results.....	163
4.4	Local Scour for Combination of Intermediate and Short Abutment.....	172
4.4.1	Development of Nonlinear Regression Model.....	173
4.4.2	Development of ANNs Models.....	175

4.4.3	Comparison of ANNs and Existing Equations .....	192
4.4.4	Sensitivity Analysis .....	193
4.4.5	Genetic Programming.....	201
4.5	Temporal Scour depth for Short Abutment .....	203
4.5.1	Development of Nonlinear Regression Model .....	206
4.5.2	Development of ANNs for Short Abutment.....	207
4.5.3	Genetic Programming.....	216
4.5.4	Sensitivity analysis .....	218
4.6	Scour hole Dimension at short abutment.....	221
CHAPTER 5 COMPLEX ABUTMENT SCOUR		
5.1	Introduction .....	225
5.2	Complex Abutment .....	225
5.3	Dimensional Analysis.....	227
5.4	Time Variation of Scour Depth around Complex Abutment .....	229
5.5	Scour Hole Development at Complex Abutment.....	242
5.6	Estimating Scour Depth at Complex Abutment .....	252
5.6.1	Scour Depth Prediction Using Effective Length .....	252
5.6.2	Scour Depth Prediction Using Regression Method.....	255
CHAPTER 6 CONCLUSION AND RECOMMENDATIONS		
6.1	Conclusions .....	258
6.2	Recommendation for Future Research .....	260
REFERENCES	.....	262

## APPENDICES

APPENDIX A Collected data from previous studies for uniform abutment

APPENDIX B FFBP and RBF Neural Network MATLAB Codes

APPENDIX C Neural Network Result for Combination of Intermediate and Short Abutment

APPENDIX D	Genetic Programming (GP) coding
APPENDIX E	FFBP Neural Network Result for Short Abutment
APPENDIX F	Time variation of scour depth at complex and uniform Abutment
APPENDIX G	Local Scour at Complex Abutment
APPENDIX H	List of Publications
APPENDIX I	CD of Movies

## LIST OF TABLES

Table 1.1	Table 1.1: Prioritized list of research and education for local scour abutment (Sturm et al., 2011)	6
Table 1.2	Table 1.2: List of improved design estimation of abutment scour depth coupled to research needs in Table 1.1(Sturm et al., 2011).	7
Table 2.1	m value for estimating of $d_{\max}$	16
Table 2.2	$C0$ and $\phi$ in terms of degree (Mirtskhoulava, 1988)	17
Table 2.3	Classification of abutments (Melville, 1992)	23
Table 2.4	Abutment shape factor (Melville, 1992)	37
Table 2.5	Flow alignment factor for different angles of attack (Melville, 1992)	38
Table 2.6	Summary of experimental data by Yanmaz and Kose (2007)	46
Table 2.7	Empirical formula to predict time dependent scour depth	48
Table 2.8	Empirical formula to estimate equilibrium time around abutment	49
Table 2.9	Empirical formula to estimate equilibrium time around abutment (Sturm 2011)	70
Table 2.10	Summary of experimental test reported by Jones et al. (1992)	74
Table 2.11	Summary of experimental test reported by Parola et al. (1996)	76
Table 2.12	Empirical equations to predict scour depth at complex pier (Parola et al., 1996)	76

Table 2.13	Summary of experimental test reported by Melville and Raudkivi (1996)	78
Table 2.14	Summary of sediment and flow details for complex pier (Coleman, 2005)	82
Table 2.15	Summary of pier and foundation details for complex pier (Coleman, 2005)	82
Table 2.16	Summary of pile details for complex pier (Coleman, 2005)	83
Table 2.17	Empirical equations to predict scour depth at complex pier (Coleman, 2005)	83
Table 2.18	Summary of sediment and flow details for complex pier (Sheppard and Renna, 2005)	86
Table 2.19	Summary of pier and foundation details for complex pier (Sheppard and Renna, 2005)	86
Table 2.20	Summary of sediment and flow details for complex pier (Ashtiani et al., 2010)	90
Table 2.21	Summary of pier and foundation details for complex pier (Ashtiani et al., 2010)	90
Table 2.22	Summary of pile details for complex pier (Ashtiani et al., 2010)	90
Table 2.23	Summary of previous studies at complex pier	93
Table 2.24	Summary of previous studies for rectangular and circular complex pier	93
Table 2.25	Summary of previous studies for complex rectangular pier with pile group	94
Table 2.26	Performance indices of various approaches for maximum scour depth (Bateni et al., 2007a)	96
Table 2.27	Comparison of various approaches to predict the equilibrium scour depth (Bateni et al., 2007a)	96
Table 2.28	Performance for BPN-ANN versus various approaches to predict the scour depth (Lee et al., 2007)	98

Table 2.29	Evaluation of various approaches for non-dimensional data set (Zounemat-kerman et al., 2009)	99
Table 2.30	Evaluation of various approaches for dimensional data set (Zounemat-kerman et al., 2009)	100
Table 2.31	Statistical properties for testing and training data set (Kaya, 2010)	101
Table 2.32	sum of square error for empirical local scour formulas and ANN (Shin and Park, 2010)	103
Table 2.33	Three best case of RBF-ANN (Begum et al., 2011)	103
Table 2.34	Comparison of RBF network with existing equation (Begum et al., 2011)	105
Table 2.35	Statistical measurement for collected data with and without coarse and non-uniform sediment (Sarлак and Sahnaz, 2011)	106
Table 2.36	Comparison of MLP and RBF-ANNs with empirical equations	107
Table 2.37	Sensitive analysis result using MLP	107
Table 2.38	Statistical properties result using GP	108
Table 2.39	Parameters of the GEP Model	109
Table 2.40	Parameters of the GEP Model	110
Table 2.41	Parameters training and testing results of LGP and ANFIS models (Güven et al., 2009)	111
Table 2.42	Statistical measurements for pier scour depths (Azamathullah et al., 2010)	112
Table 2.43	Parameters of the optimized GEP model	113
Table 2.44	A comparison of GEP and ANNs for scour abutment	113
Table 2.45	Relation between prototype and model (Novak et al., 2010)	114
Table 3.1	Velocity along the centre line of flume	119

Table 3.2	Sieve analysis results before selection	122
Table 3.3	Sieve analysis results for chosen sediment	123
Table 3.4	Dimension of abutment and foundation in Sungai Kurau (2010)	125
Table 3.5	Prototype and model dimensions in the present study	126
Table 3.6	Abutment characteristics for the present study	127
Table 3.7	Computation of $L/d_{50}$ for both abutment and foundation for present study	129
Table 3.8	Computation of $L/y$ at complex and uniform abutment	131
Table 3.9	Selected $Z$ values for abutments	140
Table 3.10	Summary of statistical properties for soft computing methods	159
Table 4.1	Empirical formula to predict time dependent scour depth	162
Table 4.2	Flow characteristics for uniform abutment in the present study	164
Table 4.3	Time variation of scour depth for AB-I , AB-II and AB-III	164
Table 4.4	Range of combined data sets from present and previous studies	171
Table 4.5	Range of data for training and testing intermediate and short abutment	172
Table 4.6	Analysis of sensitivity for independent parameters	173
Table 4.7	Analysis of sensitivity for independent parameters	174
Table 4.8	Summary of two hidden layer FFBP for the non-dimension scour depth ( $ds/dse$ )	177
Table 4.9	Summary of one hidden layer FFBP for the non-dimension scour depth, ( $ds/dse$ )	178

Table 4.10	Summary of RBF method for non-dimensional data with different neurons and spread constant	180
Table 4.11	Summary of one hidden layer FFBP for dimensional scour depth (ds)	182
Table 4.12	Summary of two hidden layer FFBP for dimensional scour depth (ds)	183
Table 4.13	Summary of RBF method for dimension data with different neurons and spread constant	185
Table 4.14	Neural network results based on statistical measures	189
Table 4.15	Performance indices of various approaches to prediction of time-dependence scour (Training data)	192
Table 4.16	Sensitive analysis results for non-dimensional parameters	196
Table 4.17	Sensitive analysis results for time, length and velocity in a dimensional data set	198
Table 4.18	Sensitive analysis results for depth, standard deviation and mean sediment size in dimensional data set	199
Table 4.19	Range of combined data sets for short abutment	204
Table 4.20	Statistical properties for collected data sets	205
Table 4.21	Range of data for training and testing short abutment	206
Table 4.22	Summary of one hidden layer ANNs with different neurons and epochs	210
Table 4.23	Summary of two hidden layer ANNs with different neurons and epochs	211
Table 4.24	Summary of RBF-ANNs with different neurons and spread constant	213
Table 4.25	Neural network results based on statistical measures	215

Table 4.26	Performance indices of various approaches to predict time-dependence scour depth	217
Table 4.27	Sensitive analysis results with non-dimensional parameters for short abutment	219
Table 5.1	Abutment-Geometry Characteristics for the Present Study	226
Table 5.2	A summary experimental result at uniform and complex abutment	237
Table 5.3	Summary of Experimental Results for present Study	247
Table 5.4	Summary of experimental data for complex pier AND ABUTMENT	251

## LIST OF FIGURES

Figure 1.1	Protection of local scour (a) Gabion; (b) Ripraps	3
Figure 1.2	Buried pile and foundation at abutments and piers (Ettema et al., 2011)	4
Figure 1.3	Exposed foundation and pile after failure at part of abutment in	4
Figure 2.1	Shields diagram (Melville and Coleman, 2000)	13
Figure 2.2	Shields diagram for uniform sediment (Henderson, 1988)	14
Figure 2.3	General Contraction and Local scour at Bridge (Melville and Coleman, 2000)	18
Figure 2.4	Time-variation of clear-water and live-bed scour	20
Figure 2.5	Local scour as a function of velocity and time (Melville and Coleman, 2000)	21
Figure 2.6	Location of abutment in channel (Melville, 1995)	22
Figure 2.7	Flow structures around abutment (Kwan, 1987)	24
Figure 2.8	Flow structure around long abutment	25
Figure 2.9	Flow pattern around long abutment (Melville, 1997)	26
Figure 2.10	Flow structure generated by compound channel including macro-turbulence (Ettema et al., 2010)	26
Figure 2.11	Effect of flow velocity on scour depth (Dongol, 1994)	30
Figure 2.12	Variation of scour depth at abutment (Barbhuiya and Dey, 2004)	30
Figure 2.13	Effect of abutment length on scour depth (Melville, 1992)	31
Figure 2.14	Variation of scour depth at abutments with the flow depth (a) Melville 1997; (b) Barkdoll et al. (2007)	32

Figure 2.15	Variation of the scour depth with flow depth (Barbhuiya and Dey, 2004)	33
Figure 2.16	Effect of sediment coarseness on the scour depth	35
Figure 2.17	Effect of sediment on the scour depth a) uniform sediment; b) non-uniform sediment (Melville, 1997)	35
Figure 2.18	Effect of sediment non-uniformity on scour depth	36
Figure 2.19	Variation of local scour with abutment alignment (Melville, 1992)	39
Figure 2.20	Case of local scour at abutment in compound channel	41
Figure 2.21	Variation of KG with approach channel geometry	42
Figure 2.22	Comparison of Yanmaz and Kose's equation (Eq.2.25) with other empirical equations (Yanmaz and Kose, 2007)	47
Figure 2.23	Definition sketch for compound channel (Sturm 2004)	53
Figure 2.24	Comparison of measured and predicted scour depth using the Equation (2.44) (Sturm,2004)	53
Figure 2.25	Comparison of measured and computed scour depth at vertical-wall using the Lim's equation (Lim, 1997)	56
Figure 2.26	Comparison of measured and computed scour depths at various abutment shapes using the Lim's equation (Lim, 1997)	57
Figure 2.27	Comparison of measured and computed scour depth at abutment with non-uniform sediment using the Lim's equation (Lim, 1997)	57
Figure 2.28	Figure 2.28: Variation of $bs / (Ks_{bd})$ in terms of $\left(\frac{L}{b_d}\right)^{2.7} \left(\frac{U}{\sqrt{gd_{50}(S-1)}}\right)$ (Kothyari and Raju, 2001)	61
Figure 2.29	Comparison between observed and compute maximum scour depth at abutment (Kothyari and Raju, 2001)	62

Figure 2.30	Comparison between observed and compute the maximum scour depth at abutment (Dey and Barbhuiya, 2004)	63
Figure 2.31	Variation of $ds/y$ with $L/y$ (Fael et al., 2006)	64
Figure 2.32	Definition for pressure flow near a bridge abutment (Briaud et al., 2009)	65
Figure 2.33	Comparison of scour depth clay between predicted and observed data in Porcelain (Briaud et al., 2009)	66
Figure 2.34	Abutment with erodible embankment (Ettema, 2010)	67
Figure 2.35	Variation of scour depth ratio in terms of discharge per unit width ratio (Ettema et al., 2010)	68
Figure 2.36	Comparison of scour depth between rigid and erodible embankment (Sturm et al., 2011)	68
Figure 2.37	Complex pier configuration suggested by Melville and Raudkivi (1996)	71
Figure 2.38	Variation of scour depth at complex pier in terms of foundation level, $Z$ (Melville and Raudkivi, 1996)	72
Figure 2.39	Complex rectangular foundation and pier (Jones et al., 1992)	73
Figure 2.40	Comparison of prediction factor for three proposed method	75
Figure 2.41	Parameters characterizing pier and foundation (Parola et al. 1996)	75
Figure 2.42	Effects of Relative Foundation Elevation and Relative Rectangular	77
Figure 2.43	Scour depth data plotted in terms of effective pier diameter (Melville and Raudkivi, 1996)	79
Figure 2.44	Complex pier supported by piles configuration (Coleman, 2005)	80
Figure 2.45	Pier components exposed with varying pile-cap elevation (suggested by Coleman, 2005)	81

Figure 2.46	Variation of local scour with pile-cap elevation (Coleman, 2005)	82
Figure 2.47	Variation of effective diameter with pile-cap elevation at complex pier (Coleman, 2005)	83
Figure 2.48	Complex pier composed of pier, foundation (pile cap) and pile group (Sheppard and Renna, 2005)	84
Figure 2.49	Effective diameters for components at complex pier	85
Figure 2.50	Three case for complex pier (Sheppard and Renna, 2005)	86
Figure 2.51	Three position for complex pier at case 1 (Sheppard and Renna, 2005)	87
Figure 2.52	Comparison between Sheppard equation and HEC-18 (Sheppard and Renna, 2005)	87
Figure 2.53	Comparison between Sheppard's equation and HEC-18 at complex pier scour (Zevenbergen, 2010)	88
Figure 2.54	Comparison between Sheppard's equation and Melville's equation at complex pier scour (Zevenbergen, 2010)	88
Figure 2.55	Comparison between Melville's equation and HEC-18 at complex pier scour (Zevenbergen, 2010)	88
Figure 2.56	Complex pier-geometry characteristics (Ashtiani et al., 2010)	89
Figure 2.57	Seven case for complex pier due to pile-cap location (Ashtiani et al., 2010)	89
Figure 2.58	The scour depth at complex pier as a function of $Z$ (Ashtiani et al., 2010)	92
Figure 2.59	Comparison of the observed and predicted scour depths at complex pier (a) Coleman's procedure; (b) Ashtiani et al.'s procedure (Ashtiani et al., 2010)	92
Figure 2.60	Error variation for MLP and RBF networks in terms of (a) MAE and (b) RMSE.	97
Figure 2.61	Configuration of BPN neural network (Lee et al., 2007)	98

Figure 2.62	Configuration of ANN model (Kaya, 2010)	101
Figure 2.63	Architecture of neural network recommended by Shin and Park (2010)	102
Figure 2.64	Verification of ANN method (Shin and Park, 2010)	102
Figure 2.65	accuracy of different method (Shin and Park, 2010)	103
Figure 2.66	Comparison between RBF network predicted and observation of scour depth (a) Training; (b) Testing (Begum et al., 2011)	104
Figure 2.67	ANN architecture with 3 neurons in hidden layer (Sarlak and Sahnaz, 2011)	105
Figure 2.68	Observed versus predicted relative scour depths by GP (Azamathullah et al., 2008)	108
Figure 2.69	Comparison of observed and measured scour depth for testing data (Guvén and Gunal, 2008)	110
Figure 2.70	Comparison of observed and measured scour depth for training data	110
Figure 2.71	Comparison of observed and proposed models for training data at pile (Guvén et al., 2009)	111
Figure 3.1	0.6 m wide rectangular flume	117
Figure 3.2	Longitudinal section of the 6.0 m long flume	117
Figure 3.3	Downstream flume Plaxiglas Gate	118
Figure 3.4	Velocity profile at different locations along center line of flume	120
Figure 3.5	Different sections to find full flow development location	120
Figure 3.6	Sand bed preparation in the test section	121
Figure 3.7	Grain size distribution (sieve analysis) before selection	122
Figure 3.8	Grain size distribution (sieve analysis) for chosen sediment	123

Figure 3.9	A sample of sediment	124
Figure 3.10	Bridge abutment and foundation in the Sungai Kurau	126
Figure 3.11	Complex abutment characters	127
Figure 3.12	Complex abutment a) FA 21; b) FA 33;c) FA 42 d) FA 43	128
Figure 3.13	Uniform abutment a) AB-I; b) AB-II; c) AB-III	128
Figure 3.14	Nixon flow meter (Streamflo)	130
Figure 3.15	Baffles at the upstream end of the flume	130
Figure 3.16	V-notch weir at the downstream of flume with $p_1=40$ cm , $B_1= 60$ cm and $h_{1max}=12$ cm	131
Figure 3.17	Detail of V-notch weir suggested by USBR standard	132
Figure 3.18	Values of $K_h$ and $C_e$ for fully contracted V-notch weirs (USBR, 2001)	133
Figure 3.19	$C_e$ value for no fully developed 90o V-notch weirs (From British Standard 3680: Part 4A and ISO/TC 113/GT 2 (France-IO) 1971)	133
Figure 3.20	Camera inside abutment to record time variation of scour depth	135
Figure 3.21	Location of maximum scour depth	136
Figure 3.22	A sample of variation of scour depth with time	136
Figure 3.23	Record the scour hole topography by camera	137
Figure 3.24	A sample of scour hole (second camera)	137
Figure 3.25	Point gauge to measure scour topography	138
Figure 3.26	Foundation-geometry characteristics	140
Figure 3.27	Sediment recess before experiment	141
Figure 3.28	Architecture of Feed Forward Neural Network	147

Figure 3.29	Architecture of Radial Basis Function Network	149
Figure 3.30	The structure of an evolutionary algorithm.	151
Figure 3.31	A simple example of a GP individual tree representing	152
Figure 3.32	The five major preparatory steps of GP (Koza et al., 2003)	153
Figure 3.33	Mutation in genetic programming	155
Figure 3.34	Crossover in genetic programming	156
Figure 4.1	Abutment and flume characteristics	163
Figure 4.2	time variation of scour depth at uniform abutments	165
Figure 4.3	Development of scour hole around AB-III	167
Figure 4.4	Equilibrium scour hole for abutment AB-III, dse=11.8 cm	168
Figure 4.5	Equilibrium scour hole a) AB-II, dse=9.5cm; b) AB-I, dse=6.7cm 3D scour hole topography around short abutment	168
Figure 4.6	3D scour hole topography around short abutment	168
Figure 4.7	Variation of scour depth with time between present data and previous studies a) normal scale; b) logarithmic scale	169
Figure 4.8	Comparison between observed and pr	175
Figure 4.9	Result of two hidden layer neural network with 11 neurons in each hidden layer and epoch=2000 for non-dimensional data (a) Training; (b) Testing	179
Figure 4.10	Result of RBF neural network with 58 neurons in hidden layer and Spread constant=0.8 for non-dimension data (a) Training; (b) Testing	181
Figure 4.11	Result of two hidden layer neural network with 9 neurons in each hidden layer and epoch=2000 for dimensional data (a) Training; (b) Testing	184
Figure 4.12	Error variations of FFBP and RBF networks for non-dimensional data in terms of a)MAE; b)RMSE	187

	(testing data)	
Figure 4.13	Error variations of FFBP and RBF networks for non-dimensional data in terms of a)MAE; b)RMSE (training data)	188
Figure 4.14	Error variations of FFBP and RBF networks for dimensional data in terms of a)MAE; b)RMSE (testing data)	190
Figure 4.15	Error variations of FFBP and RBF networks for dimensional data in terms of a)MAE; b)RMSE (training data)	191
Figure 4.16	Comparison between two hidden layer FFBP and other equations for non-dimensional data a) ANNs and Coleman et al.(2003); (b) ANNs and Ballio and Orsi (2001)	194
Figure 4.17	Sensitivity analysis for non-dimensional variable in terms of number of neurons and RMSE	197
Figure 4.18	Sensitivity analysis for non-dimensional variable in terms of number of neurons and MAE	197
Figure 4.19	Sensitivity analysis for dimensional variable in terms of number of neurons and RMSE	200
Figure 4.20	Sensitivity analysis for dimensional variable with more details	200
Figure 4.21	Comparison between observed data and GP prediction	202
Figure 4.22	Comparison between observed and predicted data using nonlinear regression	207
Figure 4.23	Result of one hidden layer neural network with 14 neurons in hidden layer and epoch=4000 (a) Training; (b) Testing	208
Figure 4.24	Result of two hidden layer neural network with 8 neurons in each hidden layer and epoch=4000 (a) Training; (b) Testing	209
Figure 4.25	Result of RBF neural network with 16 neurons hidden layer and Spread constant=0.7 (a) Training; (b) Testing	212

Figure 4.26	Variation of MAE error in testing data for FFBP and RBF networks	214
Figure 4.27	Comparison between two hidden layer ANNs with 8 neurons and Coleman et al. (2003)	216
Figure 4.28	Comparison between GP and Ballio and Orsi (2001)	218
Figure 4.29	Sensitivity analysis in terms of number of neurons and RMSE for short abutment	220
Figure 4.30	Sensitivity analysis in terms of number of neurons and MAE for short abutment	220
Figure 4.31	Scour hole topography around AB-III	221
Figure 4.32	Longitudinal profile of scour hole for a) AB-I; b) AB-II	222
Figure 4.33	Scour hole around AB-III abutment	223
Figure 4.34	Scour hole around AB-I, AB-II and AB-III in different longitudinal section	224
Figure 4.35	Scour hole around AB-III	224
Figure 5.1	Three cases for complex abutment due below the initial bed level	226
Figure 5.2	Scour depth development for FA 42 (a) NORMAL scale; (b) Logarithmic scale	230
Figure 5.3	Observed scour area development for FA 42 in Z=3 cm	231
Figure 5.4	Scour depth development for FA 21 (a) NORMAL scale; (b) Logarithmic scale	233
Figure 5.5	Scour depth development for FA 43 (a) normal scale; (b) Logarithmic scale	234
Figure 5.6	Scour depth development for FA 33 (a) NORMAL scale; (b) Logarithmic scale	235
Figure 5.7	Scour depth development for Z=1 cm (a) NORMAL scale; (b) Logarithmic scale	238
Figure 5.8	Scour depth development for Z=3 cm (a) NORMAL	239

	scale; (b) Logarithmic scale	
Figure 5.9	Scour depth development for $Z=5$ cm (a) Normal scale; (b) Logarithmic scale	240
Figure 5.10	Scour depth development for $Z=7$ cm (a) NORMAL scale; (b) Logarithmic scale	241
Figure 5.11	Observe scouring around FA 43 for $Z=1$ cm	242
Figure 5.12	Observe scouring around FA 42 for $Z=1$ cm	243
Figure 5.13	Observe scouring around FA 33 for $Z=1$ cm	244
Figure 5.14	Observe scouring around FA 21 for $Z=0$ cm	245
Figure 5.15	Scour depth as a function of top elevation of foundation	248
Figure 5.16	Scour depth as a function of top elevation of foundation	251
Figure 5.17	Variation of effective length in terms of top elevation of foundation	254
Figure 5.18	Comparison of scour-depth in terms of effective length and experimental data	255
Figure 5.19	Prediction of scour depth using regression method	256
Figure 5.20	Comparison between observed and predicted data using regression method (Equations 5.15 to 5.17)	257

## LIST OF SYMBOLS

$a_f$	foundation width
$a_p$	pier width at complex pier
$a_f$	pile-cap width at complex pier
$B$	abutment width
$B_f$	foundation width at complex abutment
$B_u$	extension of foundation at abutment upstream
$B_m$	channel width
$b_i$	bias
$b_p$	pile width at complex pier
$b_{pg}$	equivalent width of pile group
$b_s$	analogous pier diameter
$C_{Da}$	abutment drag coefficient
$C_e$	effective discharge coefficient in V-notch weir
$D_e$	effective diameter of the complex pier
$D_f$	foundation diameter
$D_p$	pier diameter
$D_{pier}^*$	effective diameter of pier
$D_{pc}^*$	effective diameter of pile cap
$D_{pg}^*$	effective diameter of pile group
$D_{eR}$	equivalent cylindrical-pier diameter
$d_{50}$	particle median diameter [m]
$d_{50a}$	particle median diameter for armoured layer

$d_I$	distance from the water surface to the low chord of the bridge
$d_{deck}$	thickness of the bridge deck
$d_{se}$	equilibrium scour depth
$d_s$	scour depth at time $t$
$d_{sf}$	maximum scour depth at foundation
$F_d$	sediment Froude number
$Fr_f$	Froude number of the approach flow on the floodplain
$Fr_{fc}$	critical approach Froude number for flow on the floodplain
$Fr_{ab}$	Froude number at the toe of abutment;
$Fr_c$	critical Froude number at the toe of abutment
$f_{cb}$	extension width of pile cap face out from column face at complex pier
$f_{cl}$	extension length of pile cap face out from column at complex pier
$f_{pb}$	extension width of pile cap face out from nearest pile centreline
$f_{pl}$	extension length of pile cap face out from nearest pile centreline
$g$	gravity acceleration
$h_e$	effective head in V-notch weir
$K_d$	sediment size factor
$K_G$	channel geometry factor
$K_I$	flow intensity factor
$K_p$	pressure flow factor
$K_s$	abutment shape factor
$K_{sh,f}$	foundation shape factor

$K_{sh,p}$	pier shape factor for
$K_t$	scour time factor
$K_{yl}$	depth-size factor
$K_\theta$	abutment alignment factor
$K_s^*$	adjusted shape factor
$K_\theta^*$	adjusted alignment factor
$L$	abutment length
$L_f$	foundation or pile-cap length
$L_R$	$L^{2/3} y^{1/3}$
$L_p$	pier length at complex pier
$L_e$	effective length at complex abutment
$L^*$	width of the flood channel
$M$	discharge contraction ratio
$m$	number of pile rows at complex pier
$n_c$	manning roughness coefficients for the main channel
$n$	number of pile columns at complex pier
$n_f$	manning roughness coefficients for the flood channel
$Q_0$	portion of the approach flow in the bridge opening
$Q_T$	total flow rate
$O_i$	observed values,
$\bar{O}_i$	average of predicted
$q_1$	unit discharge at flow approach section
$q_2$	unit discharge at bridge section
$q_{f1}$	discharge per unit width at approach section of floodplain
$q_{f2}$	discharge per unit width in contracted of floodplain

$SS_E$	sum of square error
$S_s$	density ratio
$T$	pile-cap thickness at complex pier
$T_d$	dimensionless time = $t \sqrt{\Delta g d_{50}} / L_R$
$T_s$	dimensionless time parameter = $t d_{50} \sqrt{\Delta g d_{50}} / L^2$
$T^*$	time when scour depth is equal to $0.632 d_s$
$t$	time
$t_e$	equilibrium time
$t_i$	predicted value
$U$	mean approach velocity
$U_{ab}$	velocity at toe of abutment
$U_{fl}$	velocity and at approach cross section
$U_{fc}$	critical approach flow velocity on the floodplain
$U_c$	critical velocity
$U_c^*$	critical shear velocity
$U_{ca}^*$	critical velocity for armoured layer
$U_p$	averaged flow velocity upstream of the pier
$U_{x0c}$	critical velocity in floodplain for setback abutment
$w_{ij}$	connection weight at neural network
$y^*$	flow depth in the flood channel
$y_{fl}$	flow depth at approach cross section
$Z$	top foundation elevation relative to bed level
$Z_e$	equivalent foundation high
$\sigma_g$	standard deviation of the sediment

$\tau_c$	critical bed shear-stress
$\rho$	fluid density
$\rho_s$	material density
$\nu$	kinematic viscosity
$\theta$	angle induced between the sides of the V-notch weir
$\theta_a$	angle of attack
$\theta_c$	entrainment function obtained from Shields diagram
$\phi$	angle of sediment repose
$\delta$	the average absolute error
$\beta_0, \beta_1, \beta_i$	regression coefficients
$\varepsilon$	random error (or residual)
$\tau_0$	bed shear stress of approaching flow

## LIST OF ABBREVIATION

ANFIS	Adaptive Neuron-Fuzzy Inference System
ANNs	Artificial Neural Networks
BPN	Back Propagation Neural network
CC	Correlation Coefficient
CFD	Computational Fluid Dynamic
CW	Clear Water
EA	Evolutionary Algorithm
FFBP	Feed Forward Back Propagation
FHWA	Federal Highway Administration
GA	Genetic Algorithm
GEP	Gene Expression Programming
GP	Genetic Programming
LB	live Bed
LGP	Linear Genetic Programming
MSHA	Maryland State Highway Administration
MAE	Mean Absolute Error
MLP	Multi-Layer Perception
REDAC	River Engineering and Urban Drainage Research Center
RBF	Radial Base Function
RMSE	Root Mean Square Error
SPSS	Statistical Package for the Social Sciences
USBR	U.S. Department of the Interior Bureau of Reclamation
USM	Universiti Sains Malaysia

VW Vertical Wall

WW Wing Wall

# **KESAN GEOMETRI ASAS PADA KEROKAN TEMBOK LANDAS PENDEK**

## **ABSTRAK**

Ramalan hakisan tempatan yang tepat pada penampan adalah kriteria penting dalam rekabentuk kedalaman asas jambatan yang selamat. Satu kajian eksperimen untuk meramal hakisan tempatan pada penampan seragam dan kompleks telah dijalankan. Dalam kajian ini, penampan kompleks merangkumi penampan segiempat tepat di atas asas segiempat tepat yang lebih besar saiz. Keputusan eksperimen adalah berdasarkan tiga kes hakisan. Dalam Kes I, aras asas adalah di bawah lubang hakisan. Dalam Kes II, lubang hakisan mencapai bahagian atas asas manakala dalam Kes III, bahagian atas asas adalah di dalam lubang hakisan. Keputusan menunjukkan kedalaman hakisan pada penampan kompleks adalah bergantung kepada aras asas ( $Z$ ), panjang penampan ( $L$ ) dan dimensi asas ( $L_f$ ) di samping faktor lain yang juga mempengaruhi kedalaman hakisan tempatan pada penampan berkeratan rentas seragam. Beberapa formula telah diterbitkan melalui dua kaedah, iaitu “Multiple Linear Regression (MLR)” dan panjang berkesan, untuk meramal kedalaman hakisan di sekeliling penampan kompleks. Pola pembentukan kedalaman hakisan melawan masa di sekeliling penampan kompleks juga dikaji. Untuk penampan seragam, variasi dan perubahan dimensi hakisan tempatan dengan masa dikaji. Kaedah MLR, “genetic programming (GP)” dan “artificial neural networks (ANNs)”, “feed forward back propagation (FFBP)” dan “radial basis function (RBF)” digunakan untuk meramal variasi kedalaman hakisan dengan masa pada penampan seragam. Keputusan

menunjukkan dimensi lubang hakisan pada arah-x (selari dengan aliran) adalah di antara 3L ke 5L di hulu dan hilir penampan masing-masing dan 4L pada arah-y. Analisis statistik menunjukkan walaupun kaedah ANN memberikan keputusan yang lebih baik berbanding kaedah GP dan MLR, manakale kaedah GP dan MLR adalah lebih praktikal. Analisis sensitiviti menunjukkan hakisan tempatan adalah amat dipengaruhi oleh tiga parameter yang dikaji menurut urutan berikut, nisbah masa ( $t/t_c$ ) > nisbah panjang penampan ( $L/y$ ) > nisbah halaju ( $U/U_c$ ).

# **EFFECT OF FOUNDATION GEOMETRY ON SHORT ABUTMENT SCOUR**

## **ABSTRACT**

Accurate prediction of the local scour at abutments is an important criterion to design a safe depth for the bridge foundation. An experimental study for predicting local scour around the complex and uniform abutment under clear water conditions is presented. In this research, a short complex abutment included a rectangular abutment and situated on a larger rectangular foundation. The results are presented according to three scour cases. In Case I, the foundation level was located below the scour hole. In Case II, scour depth reaches the top of the foundation, and in Case III, the top of the foundation was located within the scour hole. The results reveal that the scour depth at a complex abutment is dependent on foundation level ( $Z$ ), length of abutment ( $L$ ) and the dimensions of the foundation ( $L_f$ ) in addition to the factors that influence local scour depth at a uniform cross section abutment. Several equations have been developed based on two methods, Multiple Linear Regression (MLR) and effective length, to predict scour depth around a complex abutment. The trend of scour depth development over time around a complex abutment was also investigated. For uniform abutments, the dimension and variation of local scour with time were investigated. The MLR, genetic programming (GP) and artificial neural networks (ANNs), feed forward back propagation (FFBP) and radial basis function (RBF) were used to predict the time variation of scour depth at uniform abutment. Results indicated that the dimension of scour hole in the x-direction (parallel to flow

direction) was ranged from  $3L$  to  $5L$  in upstream and downstream of abutment respectively, and also  $4L$  in the  $y$ -direction. Statistical analysis showed that, although the ANNs technique produced better results in comparison with GP and MLR techniques, but the GP and MLR are more practical methods with formula . A sensitivity analysis indicated that the local scour greatly affected by the three studied parameters as following order, time ratio ( $t/t_c$ ) > abutment length ratio ( $L/y$ ) > velocity ratio ( $U/U_c$ ).

# CHAPTER 1

## INTRODUCTION

### 1.1 Background

Hydraulic structures generally are constructed in rivers and usually they are like an obstruction in front of flow. In the vicinity of the hydraulic structure, localised scour or erosion may occur. Scour can be defined as a digging and sediment removal around hydraulic structures and river bed. Usually scouring can be divided into local scour and general scour. Scouring due to constriction, scour in a bend of the river and bed river erosion is general scour. Local scour occurs due to the direct impact of flow to structures, for instant scour around abutment and pier or jets.

Bridges are the main structures in transportation especially during floods, but unfortunately major damage appears at bridge foundations because of scour during flood periods. One thousand bridges have collapsed over the last 30 years in the United States and 60 percent of those failures are due to hydraulic failure including bridge foundation scour (Shirole 1991). Bridge failure results in the loss of lives and financial losses for reconstruction and rehabilitation. In 1987, the collapse of the New York State Thruway bridge resulted in the loss of ten lives. When a section of the US 51 bridge fell into the Hatchie River near Covington, Tennessee, eight people were killed in 1989. Two people were killed in 1989 due to the collapse of spans of a bridge in the Great Miami River near Miami town, Ohio. In 1995, seven people were killed due to the collapse of the Interstate 5 bridges over Arroyo Pasajero in California (Miller, 2003). The total financial loss to the Georgia Department

of Transportation was approximately USD 130 million because more than 100 bridges had to be replaced and repaired due to flooding from tropical storm Alberto in Georgia in 1994 (Richardson and Davis, 2001). On average every year one bridge failure can be assigned to scour problem in New Zealand (Melville and Coleman, 2000).

Malaysia experience very high rainfall intensity, especially during the Monsoon months of December and January. The Public Department Malaysia (PWD) is the custodian of over 6,000 bridges in the country. The PWD reported that the scour is a major cause of the failure of bridge abutment and pier (PWD, 1995).

The presence of abutments in front of flow may cause a huge change in the flow pattern. The scour hole around abutment is developed due to complex vortex flow. This vortex flow develops a scour hole in three parts, in front of, to the side of, and downstream of the abutment (Dey and Barbhuiya, 2005). Numerous studies have been conducted since the late 1950s on scour around bridge piers, but challenging problems remain because of difficulties in understanding the complicated flow and scouring mechanisms combined with the complex geometries of abutment or pier.

Most investigations have been carried out for abutments with uniform cross sections (continuous horizontal cross section geometry). However, due to geotechnical and financial reasons, actual bridge abutments are built on a foundation (or pile cap) with or without pile group. Similarly, most scour depth equations in the literature focus on scour around uniform abutments. The Federal Highway Administration (FHWA) recommended in its Hydraulic Engineering Circular No. 18 (HEC-18) (Richardson and Davis, 2001) a

design approach based on “The preferred design approach is to place the abutment foundation on scour resistant rock or on deep foundations such as piles”. However, during flood, water flow usually erodes scour protection such as ripraps and gabion (Figure 1.1).

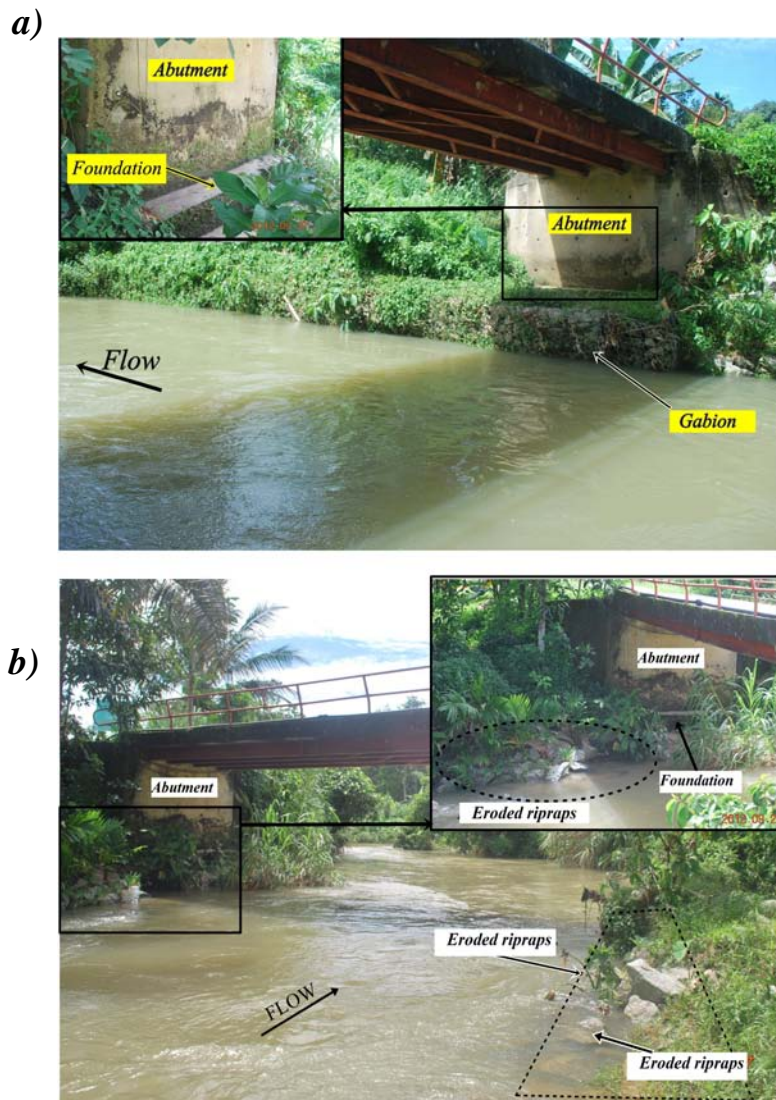


Figure 1.1: Protection of local scour (a) Gabion; (b) Ripraps

The foundation that is under the stream bed initially (Figure 1.2) may become exposed to flow due to scour caused at the abutment (Figure 1.3). Since the trend of local scour around abutments is time dependent, hence, investigation of time-dependent scouring at abutments is an important aspect to the hydraulic engineers.

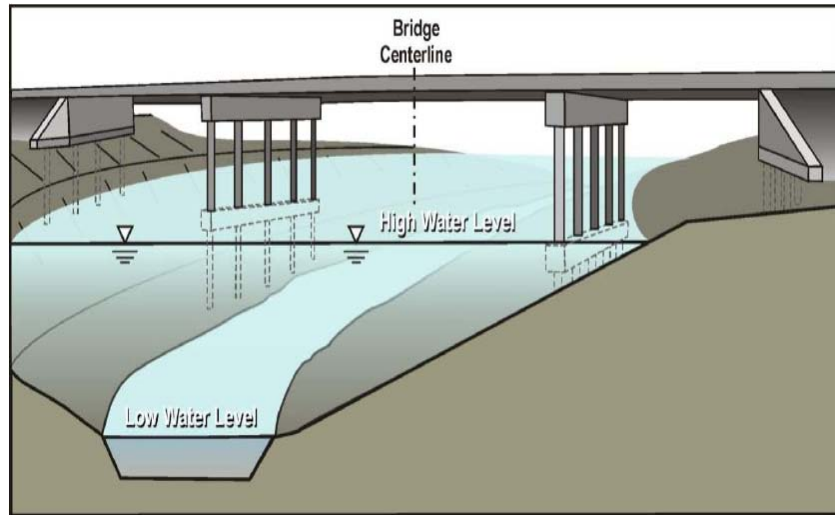


Figure 1.2 Buried pile and foundation at abutments and piers (Ettema et al., 2011)

**a)**



**b)**



Figure 1.3 Exposed foundation and pile after failure at part of abutment in a) Atlanta metro area (Sturm et al., 2011); b) Kurau River, Perak, Malaysia

## **1.2 Problem Statement**

Abutment and pier scour is the main cause of the collapse of bridges. In spite of the use of complex abutments (abutment with foundation) at river bridges, there is a lack of investigation about the effect of the foundation on scour around complex abutments, since several investigations have been undertaken on clear water scour at complex piers (Melville and Raudkivi, 1996; Melville and Coleman, 2000; Coleman, 2005; Ashtiani et al., 2010). Table 1.1 shows priorities and research topics reported by Sturm et al. (2011), investigation of realistic abutment by considering the effect of foundation is located on top of this table (L1, Table 1.1) with critical priority. Table 1.2 indicates the design-related research tasks needed to improve and validate the design methodologies which recommended for scour abutment by Sturm et al. (2011). The listed priorities in this table agree with those of given in Table 1.1.

If the effects of foundation geometry were integrated into the methods of estimation of abutment scour depth (complex abutment), the conservative approach would be unnecessary. Alternatively, abutment scour failure may be reduced by proper design of the foundation. A number of variables can have an effect on the scour depth around abutments, which the abutment length is the most important variable. There is a lack of study in literature on scour around complex abutment, the local scour included mechanism of scour, time variation of scour depth and maximum scour depth at complex abutment are investigated in this study.

Table 1.1: Prioritized list of research and education for local scour abutment  
(Sturm et al., 2011)

Aspect	Research Need	Priority
Laboratory studies	L1. Additional laboratory hydraulic experiments on realistic abutment foundation structures and abutment shapes with and without countermeasures, methods of modelling embankment material; Geotechnical stability aspects; modelling of intermediate length and short erodible embankments and wide abutments	<i>Critical</i>
	L2. Overtopping of erodible embankments and abutment scour under pressure scour conditions.	<i>High</i>
Field studies	FS1. Field studies with continuous hydraulic and scour monitoring that assess uncertainties in measurement and that can be compared with laboratory hydraulic models.	<i>Critical</i>
	FS2. An overall survey to determine the statistical distribution of embankment failure (including types of failures) relative to other modes of bridge waterway failure.	<i>Critical</i>
Numerical studies	N1. Investigation of sound use of 2D (depth-averaged models) for determining flow distribution through bridge waterways for the short term combined with 3D CFD models and laboratory turbulence measurements to shed further light on hydraulic model scaling issue for the long term.	<i>Critical</i>
	N2. Education of engineers concerning limitations of 1D abutment scour prediction formulas and the potential and applicability of 2D and 3D numerical modelling in combination with laboratory hydraulic modelling.	<i>High</i>

Table 1.2: List of improved design estimation of abutment scour depth coupled to research needs in Table 1.1(Sturm et al., 2011).

Aspect	Research Need	Design-related Research Task	Priority
Erodible embankment abutments	L1, FS1	1. Determine if and how the ABSCOUR method (MSHA, 2010) and that proposed by Ettema et al. (2010) can be merged and further developed. From diagnostic field studies determine method veracity.	Critical
	L1, FS1	2. Further develop and check the validity of the geotechnical approach to estimating scour depth. From diagnostic field studies determine method veracity.	Critical
	L1, FS1	3. Refine the methods in Task 1 for the limiting case of a short abutment as the channel becomes very wide. From diagnostic field studies determine method veracity.	Critical
	L2, FS1	4. Ascertain how the methods in Task 1 apply, or should be adjusted, for embankments under pressure scour conditions and possibly overtopping. From diagnostic field studies determine method veracity.	High
Solid body abutments	L1, FS1	5. Determine the extent to which the methods proposed by Sturm (2006) and Melville (1992, 1997) can be merged and further developed for solid-wall abutments and then combined with Task 1. In a comprehensive design procedure. From diagnostic field studies determine method veracity.	Critical
	L2, FS1	6. Ascertain how the methods in Task 5 apply,	High

		or should be adjusted, for embankments under pressure scour conditions and possibly overtopping. From diagnostic field studies determine method veracity.	
Abutments fitted with scour counter-measures	L1, FS1	7. Determine how the methods in Tasks 1 and 5 should be adjusted, for embankments fitted with scour counter-measures, notably an armoured apron around the abutment toe or sheet-pile skirt. From diagnostic field studies determine method veracity.	Critical
2-D flow numerical methods	N1	8. Utilize a 2-D flow model to determine peak values of flow velocity, unit discharge or shear stress in the vicinity of an abutment, especially if the abutment is located in a channel of irregular geometry, in order to estimate amplification of contraction scour at an abutment.	Critical

### 1.3 Objectives of the Investigation

The main objectives in this study are:

- i. To investigate the mechanism of localized scour around a complex short abutment.
- ii. To evaluate the effects of the foundation geometry on the local scour at vertical wall short abutment (complex abutment) and developing an empirical equation to predict scour depth.
- iii. To estimate time dependent processes of scour depth around uniform short abutment using Non-linear regressions, Artificial Neural Networks (ANNs) and Genetic programming methods.

## **1.4 Scope of Present Study**

This experimental research focuses on the study of local scour at short vertical wall abutment with regards to effect of foundation. All experiments were conducted at REDAC's laboratory channel under clear water and uniform flow conditions. The experiments were conducted in a simple rectangular channel with 6.0 m long, 0.6 m wide and 0.6 m deep. A number of experiments were initially conducted to make sure a fully developed boundary layer was obtained. For all experiments, uniform, non-compact and non-cohesive sand was selected. The flow depth was selected at a relatively constant depth so that no significant effect of flow depth on the scour hole is present. To maintain the clear water condition, the flow velocity was set approaching to the critical velocity of sediment. The vertical wall and short abutments were chosen in all tests, for both uniform and complex abutment. To investigate the effects of foundation elevation on a complex abutment, the foundation level was located at different levels under the initial sediment bed.

## **1.5 Thesis outline**

This thesis includes of six (6) chapters. Chapter 1 briefly introduces the research, the objectives and the scope of study.

Chapter 2 covers the literature review about the basic knowledge of local scour, the theoretical and experimental study about the prediction of the scour depth, the temporal development of abutment scour and scour depth around complex piers.

Chapter 3 expresses the research methodology which includes experimental apparatus, with the details of abutment dimensions, flume

equipments, and techniques to measure the scour depth at complex abutment. Also three techniques of Non-linear regression, ANNs, and Genetic programming (GP) are explained in this chapter.

In Chapter 4, developments of new equations for temporal scour depth at uniform short abutment are presented. The performance of traditional methods, ANNs and GP is compared using statistical analysis. At the end of this chapter, dimension of a scour hole at uniform abutment is described.

Chapter 5 presents the effect of foundation geometry on short abutment scour. Development of several new equations to predict the scour depth at complex abutment and their performances using the various statistical techniques are discussed. Time variation of scour depth around complex abutment in different foundation level is another part of this chapter.

Finally, the conclusions obtained from this research are summarized in Chapter 6. Several recommendations are also suggested for further study in the light of the present research.

## **CHAPTER 2**

### **LITERATURE REVIEW**

#### **2.1 Introduction**

Bridge failure due to scouring and stream instability problems generally has threatened the safety of highways. Scour is the result of the erosive action of flowing water excavating and transporting sediment from the banks and bed of streams. Potential scour can be a significant factor in the analysis of a stream crossing system.

Generally, scouring depends on different variables such as: erosion resistance of the material, flow power to erode and a balance between input and output sediment to section. Moveable or loose beds are rapidly eroded by flowing water while erosion-resistant materials or cement soils are more scour-resistant and in long duration process reached to final (equilibrium) scour.

One of the main requirements to design the bridge is the depth of abutment and pier foundation should be under the maximum scour depth for the worst conditions resulting from the 100-year flood, or a smaller flood if it will cause scour depth deeper than the 100-year flood. Bridge foundations should be checked to ensure that they will not fail due to scour resulting from the occurrence of a super flood in order of magnitude of a 500-year flood (Richardson and Davis 2001). Unfortunately, in spite of the significant research in scour around abutment and piers, bridges still fail due to scour. It is believed that this is due to inadequacies in both knowledge about scouring and also design criteria adopted for older bridges.

## **2.2 Sediment Transport in Rivers**

Sediment transport is the movement of solid particles (sediment), typically due to a combination of the force of gravity acting on the sediment, and/or the movement of the fluid in which the sediment is entrained. Usually the knowledge of sediment transport is most often used to determine sediment erosion and deposition, also the magnitude and time of this erosion or deposition can be determined.

A hydrodynamic force is applied to sediment particles at the river from the water. The threshold of particle (sediment) occurs when the applied forces due to flow, causes a particle to move, exceeding the stabilising force due to gravity for non-cohesive sediments. In cohesive soils where the electro-chemical force dominates between particles, then sediment size and particle weight may have less importance. The governing equations for erosion of non cohesive and cohesive sediment are discussed in this Chapter.

### **2.2.1 Uniform Non-cohesive Sediments**

Shields in 1936 (Yang, 1996) published his principle for threshold conditions of uniform sediment on a flat bed in unidirectional flow. The river bed is without any movement for flows below the incipient motion of sediment. The data which was used by Shields was founded by extrapolating curves. In rivers, sediment have non-uniform distribution, therefore Shields drew a broad belt. The critical bed shear stress (entrainment function) can be obtained from Shields diagram (Figure 2.1). The critical bed shear-stress ( $\tau_c$ )

and critical shear velocity  $U_c^*$  can be calculated for a given sediment size of  $\theta_c$ .

$$\tau_c = \rho U_c^{*2} \quad (2.1)$$

$$\theta_c = \frac{U_c^{*2}}{(S_s - 1)gd_{50}} \quad (2.2)$$

where  $\tau_c$  is critical bed shear-stress,  $\rho$  is fluid density;  $U_c^*$  is critical shear velocity;  $\theta_c$  is the entrainment function obtained from Shields diagram;  $S_s$  is density ratio ( $\rho_s/\rho$ );  $\rho$  is fluid density;  $\rho_s$  is material density;  $g$  is the gravity acceleration and  $d_{50}$  is particle median diameter.

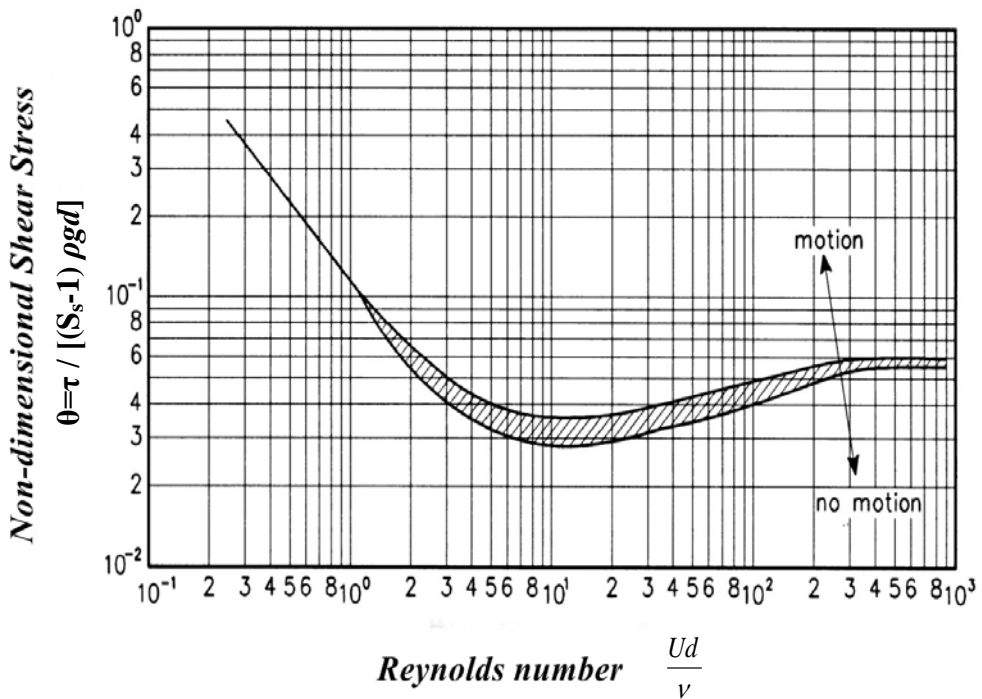


Figure 2.1: Shields diagram (Melville and Coleman, 2000)

Numerous equations exist for critical velocity for sediment movement. The logarithmic form of the critical velocity profile is suggested by Melville and Sutherland (1988) as:

$$\frac{U_c}{U_c^*} = 5.75 \log \left( 5.53 \frac{y}{d_{50}} \right) \quad (2.3)$$

where  $y$  is the flow depth,  $d_{50}$  is the mean sediment diameter and  $U_c$  is the critical velocity.

Another method to find threshold conditions for uniform sediments is through Shields diagram (Figure 2.2) as suggested by Henderson (1966). For water and sediment with densities of  $1,000 \text{ kg/m}^3$  and  $2,650 \text{ kg/m}^3$ , the critical velocity ( $U_c$ ) can be determined using Figure 2.2 and Equation (2.3) (Melville and Sutherland, 1988)

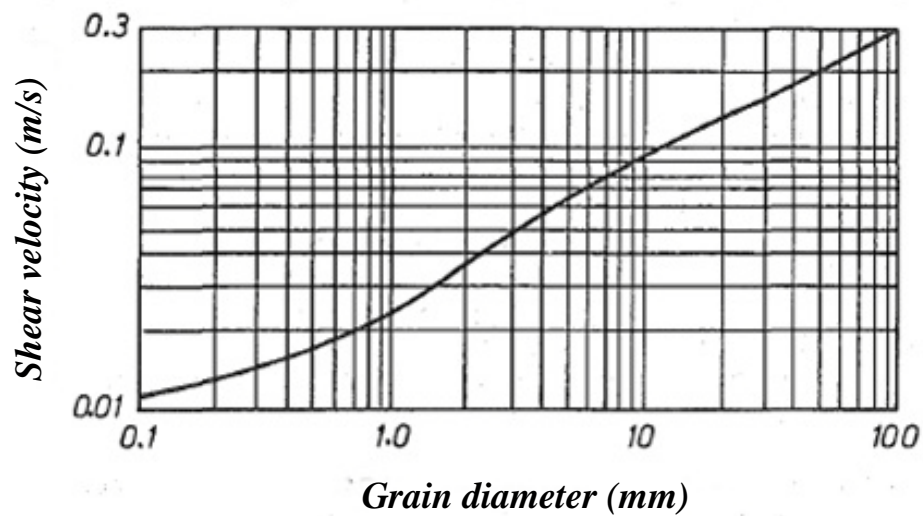


Figure 2.2: Shields diagram for uniform sediment (Henderson, 1988)

In water at  $20^\circ\text{C}$ , a useful estimation was suggested by Melville (1997) for the Shields diagram in quartz sediments as:

$$U_c^* = 0.0115 + 0.0125 d_{50}^{1.4} \quad 0.1 \text{ mm} < d_{50} < 1 \text{ mm} \quad (2.4)$$

$$U_c^* = 0.0305 d_{50}^{0.5} - 0.0065 d_{50}^{-1} \quad 1 \text{ mm} < d_{50} < 100 \text{ mm} \quad (2.5)$$

### 2.2.2 Non-uniform and Non-cohesive Sediments

For uniform bed sediments Equation (2.3) can be used to calculate  $U_c$  in the riverbed. However for non-uniform grain, the flow removes small sediment and changing others into an armoured layer. Therefore, for non-uniform materials the effects of sediment size distribution are significant and would depends on standard deviation ( $\sigma_g = d_{84} / d_{50}$ ) and mean sediment diameter (Melville and Sutherland, 1988). The mean velocity in non-uniform bed obtained from  $U_{ca}$ ; an armoured layer can be formed at flow velocity less than  $U_{ca}$  and at a velocity greater than  $U_{ca}$  armoured layer was removed. Chin (1985) showed  $U_{ca}$  depends on the standard deviation and sediment size,  $U_{ca}$  raises with increasing standard deviation for a given  $d_{50}$ . The value of  $U_{ca}$  also depends on  $d_{max}$  which can be derived from Chin's equation (Chin, 1985):

$$d_{max} = \sigma_g^m d_{50} \quad (2.6)$$

in which  $m$  depends on  $d_{max}$  as shown in Table 2.1.

The  $d_{50a}$  can be found by following equation to determine the critical shear velocity ( $U_{ca}^*$ ) in armoured layer from Shields diagram (Figure 2.2).

$$d_{50a} = \frac{d_{max}}{1.8} \quad (2.7)$$

By using  $U_{ca}^*$  and  $d_{50a}$  the value of  $U_{ca}$  can be calculated from Equation (2.3).

Table 2.1: m value for estimating of  $d_{max}$

Assumed value of $d_{max}$	m
$d_{90}$	1.28
$d_{95}$	1.65
$d_{98}$	2.06
$d_{99}$	2.34

### 2.2.3 Cohesive Sediments

In cohesive sediment large forces are necessary to rupture the aggregates within the sediments and fairly small forces are necessary to sediment transport. Mirtskhoulava (1991) illustrated that scour in clay soils occurs in several stages. In the first step, the bed roughness is developed due to separating of soil and washing by water. Afterward drag and lift forces raise the vibration and action on the protruding aggregates. The result of this process is that the bonds between aggregate are slowly cracked until the aggregate is ripped from the bed and carried away by water. Mirtskhoulava (1988) showed that the critical depth-average velocity ( $U_c$ ) for cohesive sediments can be calculated by the following equation:

$$U_c = \log\left(\frac{8.8y}{d_a}\right) \sqrt{0.4\left((S_s - 1)gd_a + \frac{0.6}{\rho} C_f\right)} \quad (2.8)$$

in which  $y$  is the flow depth;  $d_a = 0.004m$  (detaching aggregate size);  $S_s$  is density ratio ( $\rho_s/\rho$ );  $\rho$  is fluid density and  $\rho_s$  is material density;  $g$  is the gravity acceleration and  $C_f = 0.035C_0$ ;  $C_0$  can be determined from Table 2.2.

Table 2.2:  $C_o$  and  $\phi$  in terms of degree (Mirtskhoulava, 1988)

Type of soil and range of Liquidity index		Soil property at voids ratio						
		0.45	0.45	0.65	0.75	0.83	0.95	1.05
Loamy sand								
0 - 0.25	$C_o=$	14.7	10.8	7.85				
	$\phi=$	(30)	(29)	(27)				
0.25 - 0.75	$C_o=$	12.7	8.83	5.88	2.97			
	$\phi=$	(28)	(26)	(24)	(21)			
Loamy clay								
0 - 0.25 (low plasticity)	$C_o=$	46.1	36.3	30.4	24.5	21.6	18.6	
	$\phi=$	(26)	(25)	(24)	(23)	(22)	(20)	
0.25 – 0.5 ( medium plasticity)	$C_o=$	38.2	33.3	27.5	22.6	17.7	14.7	
	$\phi=$	(24)	(23)	(22)	(21)	(19)	(17)	
0.5 – 0.75 ( high plasticity)	$C_o=$			24.5	19.6	15.7	13.7	11.8
	$\phi=$			(19)	(18)	(16)	(14)	(12)
Clay								
0 – 0.25	$C_o=$		79.4	66.8	53.0	46.1	40.2	35.3
	$\phi=$		(23)	(22)	(21)	(19)	(17)	(17)
0.25 – 0.5	$C_o=$			55.9	49.0	42.2	36.3	31.4
	$\phi=$			(18)	(17)	(16)	(14)	(11)
0.5 – 0.75	$C_o=$			44.1	40.9	35.3	32.4	28.4
	$\phi=$			(15)	(14)	(12)	(10)	(7)

### 2.3 Type of Bridge Scour

An understanding of different type of river scour is important to design hydraulic structures. The process of scouring in rivers can result from human alterations or natural phenomena. The hydraulic structures cause changes to the flow patterns in the vicinity of structures, then change in flow parameters cause changes to sediment transport capacity. Then local disequilibrium transportation occurs between the capacity of flow to the sediment transport and actual sediment transport. Consequently, the local scour can be developed

around bridge pier and other structures. Type of scour at bridge cross sections can be divided into three different types; general scour, contraction scour and local scour as shown in Figure 2.3. At a bridge crossing one or all of different types of scour can occur (Melville and Coleman, 2000).

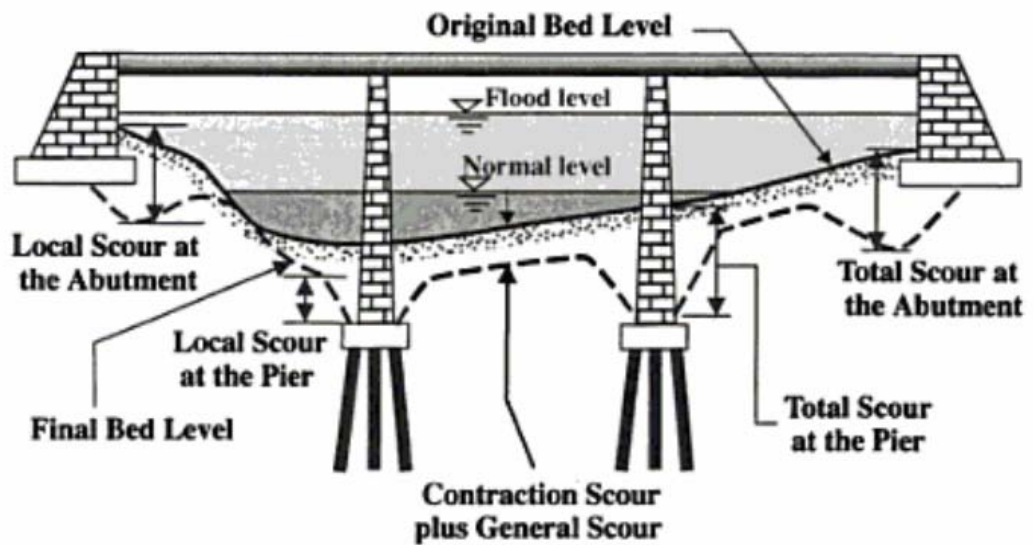


Figure 2.3: General Contraction and Local scour at Bridge (Melville and Coleman, 2000)

*General scour* is a process of geomorphologic and fluvial process in a river catchment, that results in changes in the flow conditions in form of general scour. Two types of general scour, long-term and short-term, can be recognised in bridge cross section and rivers. Long term general scour includes progressive degradation and lateral bank erosion. This kind of scour needs a long time to completely develop (generally several years or longer). Short-term general scour develops during the floods. General scour occurs irrespective of the presence of a bridge structure. But the local scour and contraction scour directly depends on the existence of the bridge.

*Contraction scour* occurs due to existence of bridge in rivers. Usually, the flow converges in vicinity of the bridge. The encroachment from the abutments causes the flow to contract, accelerating through the bridge section, then at the bridge downstream the flow gradually decelerates in the channel of the river. Due to the flow acceleration large shear stresses are exerted to the bed sediment and finally contraction scour occurs throughout the contracted section.

*Local Scour* results from impacts of flows to abutments or piers. Local scour only occurs if the local flow field has enough energy to transport the bed sediment and is characterised by the formation of scour holes adjacent to the abutment. Prototype experience and physical model testing have allowed the development of methods for forecasting and preventing scour at various structures. Local scour and contraction are both induced by the existence of the pier and abutment.

#### **2.4 Classification of Local Scour around Abutments**

Chabert and Engeldinger (1956) classified the local scour based on the mode of sediment transport into two categories, namely, clear-water and live-bed scour. Localised scour around abutment can occur either as clear-water scour or live-bed scour. It is necessary to ensure that the scour depth include is designed for all possible causes.

*Clear-water scour* occurs when the sediment is at rest in upstream of the abutment. Clear-water scour happens when the shear stress exerted on the sediment by the flow is less than the critical shear stress of the sediment. The

equilibrium scour depth (maximum scour) occurs when the flow can no longer remove sediment from the scour area.

*Live-bed scour* occurs when the bed material upstream of the abutment is being transported to scour hole, such that there is general sediment transport by the river. The live bed scour happens when the shear stress exerted on the sediment by the flow is greater than the critical shear stress of the sediment. Under live-bed conditions the local scour develops quickly and then fluctuates about the equilibrium scour depth due to propagating bed-forms (shown by the dashed lines in Figure 2.4 and Figure 2.5). Under equilibrium scour depth, time-average sediment transport into the scour hole equals that removed from scour hole.

The time-variation of clear-water and live-bed scour is illustrated in Figure 2.4. Maximum clear-water scour depth is greater than the live-bed scour depth (almost 10%).

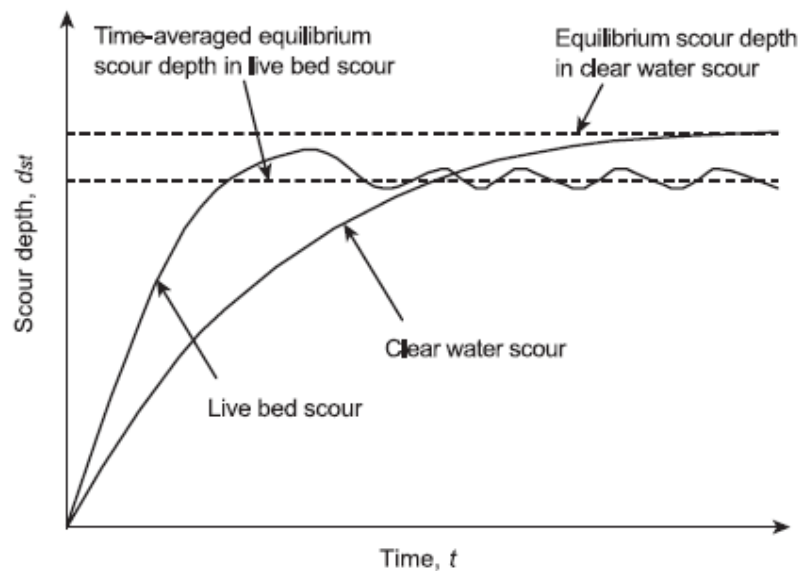


Figure 2.4: Time-variation of clear-water and live-bed scour

(Melville and Coleman, 2000)

Figure 2.5 shows development of the local scour depth as a function of flow velocity and time in clear-water and live-bed condition.

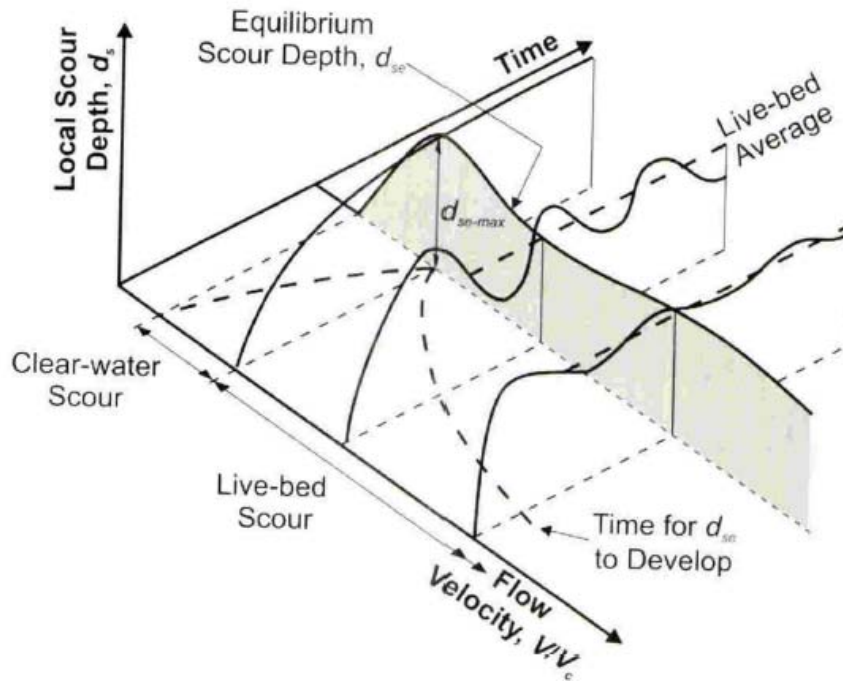


Figure 2.5: Local scour as a function of velocity and time (Melville and Coleman, 2000)

Generally, an abutment is located in the compound channel which can be included of a floodplain and main channel (Figure 2.6). Whether the scour type is live-bed or clear-water usually depends on the position of the abutment relative to the river channel. For abutments that are located on the river floodplain, during flooding, clear-water scour conditions are more likely to occur in result of the protection afforded by vegetation on the bed of the floodplain and lower flow velocities that usually occur on the floodplain. However, if the abutment is located in the main river channel, live-bed scour conditions are more likely to occur during the flood.

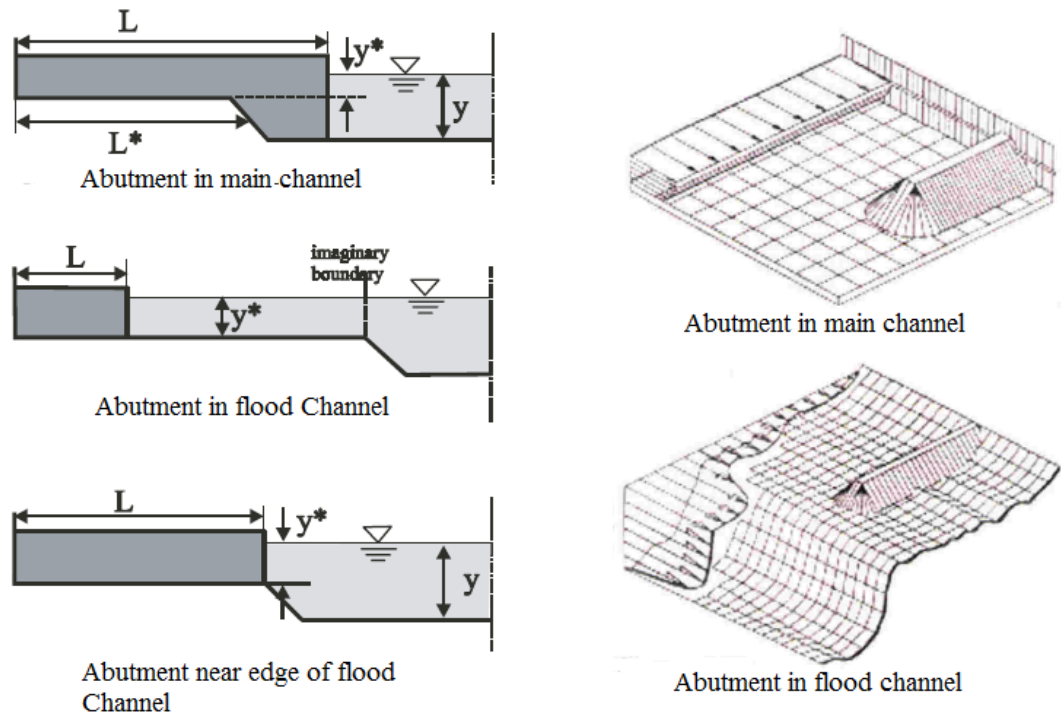


Figure 2.6: Location of abutment in channel (Melville, 1995)

## 2.5 Short Abutment and Long Abutment

The approaching flow depth is one of the main factors to determine the scour depth around abutments. Kandasamy (1989) showed the maximum scour depth increases with increase in approaching flow depth, at a decreasing rate. Melville (1992) summarized a large number of experimental results on clear-water abutment scour and proposed a design method for maximum scour depth that depends on abutment length and empirical correction factors. The abutment was classified in three groups as short abutment, intermediate abutment lengths, and long abutment (Table 2.3). The maximum clear-water scour depth is  $2L$  and  $10y$  for the short and for long abutment respectively. As shown in Figure 2.6,  $L$  and  $y$  were used for the abutment length and flow depth respectively. The equilibrium clear-water scour depth at intermediate abutment lengths can be calculated as discussed in Section 2.9.

Table 2.3: Classification of abutments (Melville, 1992)

Length ratio	Abutment Type
$L/y \leq 1$	Short abutments
$1 < L/y \leq 25$	Intermediate length abutments
$L/y > 25$	Long abutments

## 2.6 Mechanisms of Scour around Abutments

Abutment, in general, constricts the flow in a river and increases both mean velocity (in the main of channel) and local velocity near the abutment in such way that they result in a horizontal constriction with a three-dimensional flow. When water flows around the abutment, the streamlines contract near the end of the abutment as the flow accelerates past it. The local flow structure at bridge abutments depends on the length of the abutment and the obstruction shape. Various studies have been undertaken on the mechanism of scour at abutment and piers, including those given by Kwan (1987), Wong (1982), and Kwan and Melville (1994). These researchers generally showed the similarity of the flow pattern in and around the scour area, specifically where the abutment as a short obstacle expands into the channel in relation to the flow depth. At the piers, on the line of symmetry, deepest scour occurs, while in short abutment the maximum scour depth occurs in upstream and nose of the abutment.

The flow around abutment could be broken down into four components, a down-flow, primary vortex (also termed the principal vortex), secondary vortex and wake vortices (Kwan, 1987). Figure 2.7 shows the flow components around the abutment.

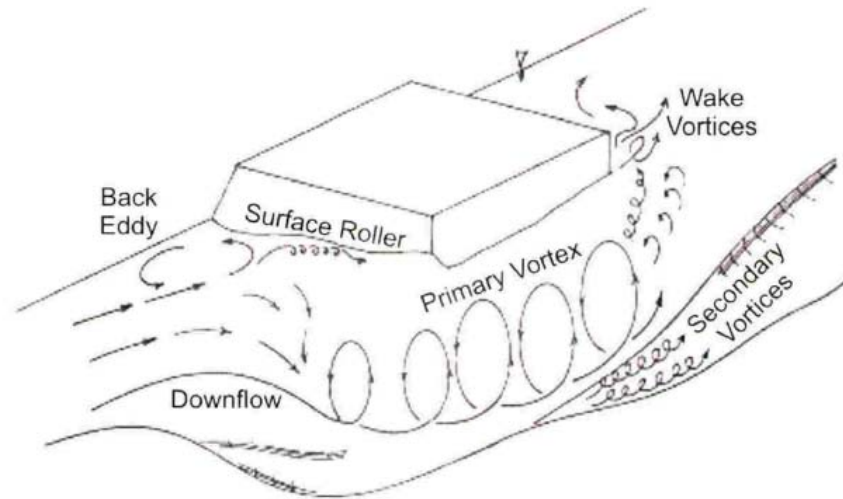


Figure 2.7: Flow structures around abutment (Kwan, 1987)

The down-flow and the primary vortex are confined mostly to scour hole under the original level of sediment (Kwan and Melville, 1994). The vortex flow and the down-flow are relatively unaffected by change of approaching flow depth. The shape of primary vortex is elliptical, with an inner core region being a forced vortex and an outer core region a free vortex. Around 17% of the area of the scour hole occupied by the inner core of the primary vortex and contains up to 78% of the total circulation in the flow. In the vicinity of abutment the maximum velocity and down-flow component are 1.35 and 0.75 times of the approaching flow velocity respectively.

The secondary vortices are tempted by the primary vortex and rotate in the opposite direction. The secondary vortices develop a smaller hole on the outside of the initial scour hole. The wake vortices form as the flow separates from the end of the abutment and is carried downstream by the channel flow. Although, it sounds that the wake vortices have insignificant effect on the scour depth, but their turbulence gives them the capacity to induce scour.